

# $G^-$ and $G^+$ in the Raman spectrum of isolated nanotube: a study on resonance conditions and lineshape

H. Telg<sup>1,\*</sup>, M. Fouquet<sup>1</sup>, J. Maultzsch<sup>1</sup>, Y. Wu<sup>2</sup>, B. Chandra<sup>3</sup>, J. Hone<sup>3</sup>, T. F. Heinz<sup>2</sup>, and C. Thomsen<sup>1</sup>

<sup>1</sup> Institut für Festkörperphysik, Technische Universität Berlin, Berlin, Germany

<sup>2</sup> Departments of Electrical Engineering and Physics, and Nanoscale Science and Engineering Center, Columbia University, New York 10027, USA

<sup>3</sup> Department of Mechanical Engineering, and Nanoscale Science and Engineering Center, Columbia University, New York 10027, USA

Received 7 July 2008, revised 29 July 2008, accepted 30 July 2008

Published online 10 September 2008

PACS 63.22.+m, 78.30.Na

\* Corresponding author: e-mail telg@physik.tu-berlin.de

We analyze the high-energy Raman modes,  $G^+$  and  $G^-$ , in a pair of one metallic and one semiconducting nanotube grown across a 100  $\mu\text{m}$  wide slit. By combining Raman resonance profiles of the radial breathing mode and the high-energy modes, we assign the broad  $G^-$  peak to a metallic and the  $G^+$  peak to a semiconducting nanotube. Considering theoretical predictions we show that both peaks,  $G^-$  and  $G^+$ , originate from the LO phonon.

The  $G^-$  peak is the longitudinal mode of the metallic tube; it is broadened and downshifted due to strong electron-phonon coupling in the metallic nanotube. The  $G^+$  peak is due to the longitudinal mode in the semiconducting tube. An asymmetric lineshape of the  $G^-$  peak agrees with observations of the asymmetry to be an intrinsic feature of metallic nanotubes.

© 2008 WILEY-VCH Verlag GmbH & Co. KGaA, Weinheim

The high-energy modes (HEM),  $G^-$  and  $G^+$ , in the nanotube Raman spectrum are the most utilized features of carbon nanotubes to distinguish between metallic and semiconducting nanotubes [1–3]. While the Raman spectrum of an ensemble of nanotubes, containing a large number of tubes with different chiral indices (n,m), always shows a sharp ( $\approx 10 \text{ cm}^{-1}$ )  $G^+$  peak at  $\approx 1590 \text{ cm}^{-1}$ , the lineshape and position of the  $G^-$  peak vary with excitation energy. When mainly semiconducting nanotubes are in resonance  $G^-$  has a similar width as  $G^+$ , and when metallic tubes are coming into resonance the intensity of  $G^-$  increases, the peak shifts to lower energies, becomes broader and symmetric. While for semiconducting nanotubes  $G^-$  and  $G^+$  have been attributed to the TO and LO phonons, respectively [4,5], the origin of these peaks in metallic nanotubes and the symmetric lineshape is still under debate [5–10].

Initially the origin of "metallic" lineshape of the HEM was assumed to be electron-plasmon coupling in metallic nanotubes [11,12]. It was suggested that in a bundle of metallic nanotubes, a continuum of plasmon states coupled to the TO phonon gives rise to the Fano lineshape, i.e., a  $G^-$  peak which is broadened, downshifted and asymmetric. Referring to this model the lineshape in an isolated nanotube should be similar to the spectrum of a semiconducting nanotube, since the continuum of plasmons is solely present in nanotube bundles. Another model predicts a strong electron-phonon coupling in metallic nanotubes [5,6]. As a result the LO-phonon is drastically downshifted below the frequency of the TO-phonon. Additionally this predicts a broad peak which is asymmetric due to the phonon coupling to the continuum of electrons close to the Fermi-level. In contrast to the model of an electron-plasmon coupling these effects should be visible in a bun-

dle of metallic nanotubes as well as an isolated metallic nanotube [9].

In this paper we present resonant Raman measurements on a small bundle of one metallic and one semiconducting nanotube. Based on resonance profiles of the radial breathing mode (RBM) we assign the tubes to the metallic (12,3)-tube and a semiconducting tube, respectively. Correlating the resonance conditions of the RBMs and the high-energy modes,  $G^+$  and  $G^-$ , we show that the  $G^-$  peak originates from the metallic and the  $G^+$  peak from the semiconducting tube. Our result of an asymmetric lineshape of the  $G^-$  peak supports the idea that the Fano lineshape is an intrinsic property of metallic nanotubes. By comparison of the high-energy mode peak positions to theoretical predictions we show that the observed  $G^+$  and  $G^-$  peaks originate from LO-phonons in semiconducting and metallic nanotubes, respectively.

Nanotubes were grown on a Silicon substrate by the chemical vapor deposition method. In a previous step an  $100\ \mu\text{m}$  wide trench was etched into the substrate so that some tubes ended up crossing the trench [13]. By keeping the catalyst density low tubes were prevented from forming bundles. Therefore most tubes crossing the trench were isolated or agglomerated in very small bundles.

Resonant Raman spectroscopy was performed on a tiny bundle of nanotubes containing one metallic and one semiconducting nanotube. Spectra were collected using a triple-monochromator Raman setup in combination with a charge-coupled device. The excitation wavelength was tuned from 1.87 to 2.15 eV using a dye laser running with Rhodamin 6G. All presented spectra were normalized to integration time, laser power and the Raman intensity of  $\text{CaF}_2$  excited at an appropriate laser energy so that the wavelengths of the scattered light match. Therefore the given intensities are proportional to the Raman susceptibility.

Figure 1 shows the low and the high-energy regime of the Raman spectrum excited at 2.04 eV, including the radial breathing modes and the high-energy modes. Two RBMs are observed at  $140\ \text{cm}^{-1}$  ( $\text{RBM}_1$ ) and  $217\ \text{cm}^{-1}$  ( $\text{RBM}_2$ ) referring to two tubes with diameters of 1.76 and 1.09 nm, respectively [14, 15]. For all excitation energies we did not observe any RBM at another position than these two. Therefore our working hypothesis is that the sample consists of only two nanotubes. The high-energy regime of the spectrum in Fig. 1 shows a lineshape which is commonly referred to as a metallic lineshape. It shows a narrow ( $\text{fwhm} = 10\ \text{cm}^{-1}$ )  $G^+$ -peak at  $1590\ \text{cm}^{-1}$  and a broad  $G^-$ -peak ( $\text{fwhm} = 49\ \text{cm}^{-1}$ ) at  $1540\ \text{cm}^{-1}$ .

Changing the excitation energy revealed that the  $G^-$  and the  $G^+$  peak have differing resonance conditions. Therefore the origin of the  $G^-$  peak is a different nanotube than the tube related to the  $G^+$  peak. This is in contrast to the common assumption for such lineshape where both peaks are attributed to metallic nanotubes. The RBM peaks also show differing resonance conditions with the reso-

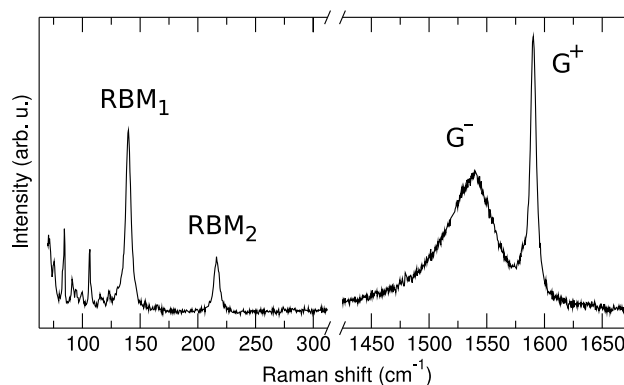


**Figure 1** Raman spectrum excited at a laser energy of 2.04 eV. Two radial breathing modes indicating the presence of at least two nanotubes. The high-energy modes show a lineshape which is commonly referred to as a metallic lineshape with a narrow  $G^+$  and broad  $G^-$  peak. We will show later that in this particular spectrum  $G^-$  is from a metallic tube and  $G^+$  from a semiconducting one.

nance condition of  $\text{RBM}_2$  ( $\text{RBM}_1$ ) being similar to that of  $G^-$  ( $G^+$ ). Therefore we assign the  $G^-$ -peak ( $G^+$ -peak) to the tube which gives rise to  $\text{RBM}_2$  ( $\text{RBM}_1$ ). To exemplify our assignment we plot in Fig. 2 the different Raman modes as a function of excitation energy. In Fig. 2 we show  $\text{RBM}_2$  ( $\text{RBM}_1$ ) on the top (bottom) right in comparison to the  $G^-$  peak ( $G^+$  peak) on the top (bottom) left.  $G^-$  is the first peak which appears starting from the smallest excitation energy. When it increases  $\text{RBM}_2$  appears and is at maximum when  $G^-$  is at maximum. At even higher energies, when the  $G^-$ -peak and the  $\text{RBM}_2$  already passed their maximum intensity, the  $G^+$  peak and  $\text{RBM}_1$  appear simultaneously and have their maxima at the same excitation energy. It is noticeable that the high-energy modes ( $G^-$  and  $G^+$ ) remain visible at higher excitation energies while the RBMs disappear after passing the resonance energy. This is due to the much larger phonon energy of  $G^-$  and  $G^+$ . A resonance Raman process involves two resonance conditions, the incoming and the outgoing resonance. While the energy of the incoming Resonance is given by the energy of the optical transition, the energy of the outgoing resonance is given by the optical transition energy plus the phonon energy (Stokes-scattering). In our case this means that the  $G^-$  peak ( $G^+$ -peak) and the  $\text{RBM}_2$  ( $\text{RBM}_1$ ) are in incoming resonance at the same excitation energy but the  $G^-$  peak ( $G^+$ -peak) remains in resonance at higher energies since the outgoing resonance is at much higher energies.

In order to assign a particular chiral indices to an observed nanotube the RBM-frequency and the optical transition energy is necessary. While the former can be obtained from almost every spectrum the latter can be obtained from a resonance profile, in our case the resonance profile of the RBM [15, 14]. For  $\text{RBM}_1$  ( $\text{RBM}_2$ ) we get a

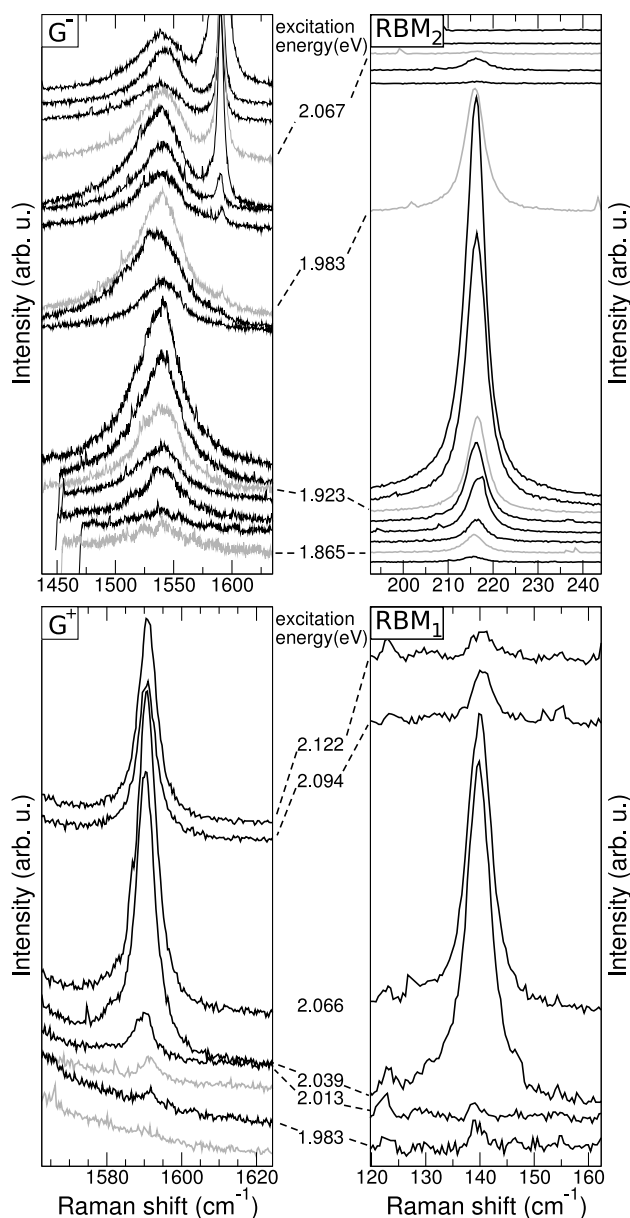


**Figure 2** Raman intensities as a function of excitation energy. Going from smaller to larger energies, the maximum intensity is reached at the same excitation energy for the  $G^-$  peak (top left) and  $RBM_2$  (top right), and the  $G^+$  (bottom left) peak and  $RBM_1$  (bottom right), respectively. The intensities of the  $G^+$  and  $G^-$  remain high at higher energies due to outgoing resonance.

RBM-frequency of  $140\text{ cm}^{-1}$  ( $217\text{ cm}^{-1}$ ) and a transition energy of  $2.042\text{ eV}$  ( $1.937\text{ eV}$ ) Finally a data point in the Kataura plot needs to be found which matches these values [16]. The Kataura plot we used is based on experiments on nanotubes dispersed in solution. The transition energies in nanotubes depend on the nanotube environment whereas the RBM frequencies hardly change [15, 17, 18]. Assuming a downshift of the transition energy due to the different

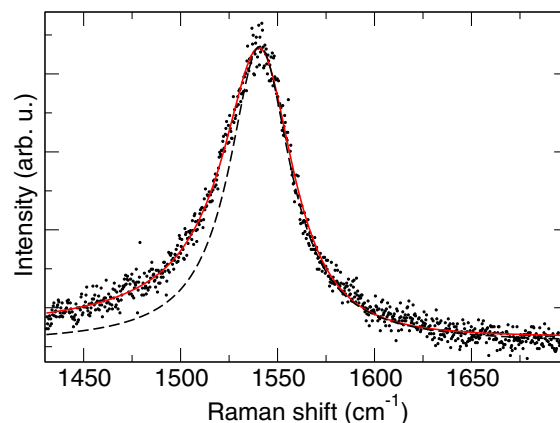


**Figure 3** Raman spectrum excited at  $1.9678\text{ eV}$ . The red graph shows a fit of the Fano-lineshape (Eq. (1)). We added a symmetric Lorentzian (dashed line) to emphasize the asymmetry of the peak.

environment - the nanotubes observed in this work are exposed to air - we assign  $RBM_2$  and therefore  $G^-$  to a tube in the (13,1) branch, whose members are all metallic nanotubes. Since it fits our data the best we assign  $RBM_2$  to the (12,3) nanotube.  $RBM_1$  thus  $G^+$  cannot unambiguously be assigned to a particular nanotube index. In the Kataura plot  $RBM_1$  is located right between the 3rd and 4th optical transition of semiconducting nanotubes.

Now that we know that the origin of the  $G^-$  peak is a single metallic nanotube we want to study the lineshape of the  $G^-$  peak. In Fig. 3 we show the  $G^-$  peak of the metallic nanotube excited at  $1.968\text{ eV}$ . The lineshape of the  $G^-$  peak is slightly asymmetric. To emphasize the asymmetry we added a symmetric Lorentzian (dashed line) to the plot in Fig. 3. The solid line, which gives a good description of the experimental data, is obtained when fitting the spectrum with a Fano-lineshape [19, 20],

$$I(\omega) = A \cdot \frac{[1 + 2\frac{\omega - \omega_P}{q\Gamma}]^2}{1 + [2\frac{\omega - \omega_P}{\Gamma}]^2} \quad (1)$$

Here  $A$ ,  $\Gamma$  and  $\omega_P$  are, respectively, the line strength, the full width at half maximum (fwhm) and the phonon frequency of the  $G^-$  peak.  $q$  represents the magnitude of the peak asymmetry. The mechanism which can give rise to a Fano-lineshape is an interaction between a discrete state and a continuum. The first who suggested the asymmetry to be of Fano-type were Brown *et al.* [11], who proposed the a coupling between the  $G^-$  mode and a continuum of plasmons. Kempa *et al.* [12] showed that the plasmon continuum results from the bundling of metallic tubes and should therefore not exist in isolated metallic tubes. Therefore we favor a proposal by Lazzeri *et al.* [6]. They suggest a coupling of the  $G^-$  mode phonon to the continuum of electronic states close to the Fermi-level to be the origin of the Fano-lineshape in metallic carbon nanotubes [6, 9].

In the following section we assign the high-energy modes of the metallic and the semiconducting nanotube to

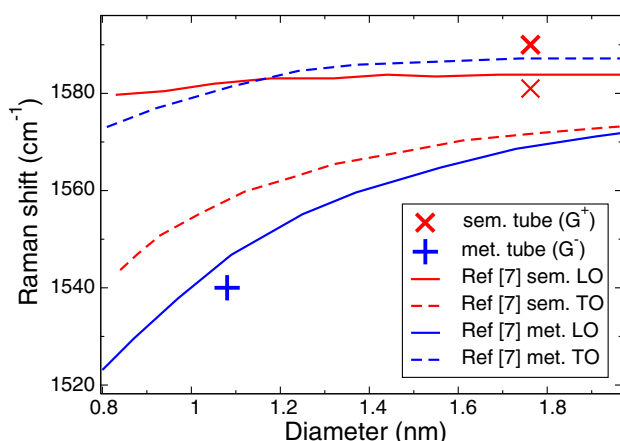


**Figure 4** High-energy mode frequencies ( $G^-$  and  $G^+$ ) as a function of tube diameter. The  $G^-$  peak (blue plus symbol) which we assigned to the metallic tube matches theoretical results for LO-phonons in metallic nanotubes. The  $G^+$  peak (large red x symbol) with its weak shoulder (small x symbol) referring to the semiconducting tube is  $\approx 10 \text{ cm}^{-1}$  higher than the theoretical predictions for LO and TO phonons in semiconducting tubes. Theoretical data are taken from Ref. [7]

a particular phonon-mode. Therefore we compare the observed phonon energies as a function of tube diameter to *ab initio* calculations of phonon dispersion relations [7]. Figure 4 shows the theoretical data from Ref. [7] of the TO (dashed line) and the LO (solid line)  $\Gamma$ -point phonons. In case of LO phonons they observed a tremendous deviation between metallic (open circle) and semiconducting (filled circle) tubes. The origin of this deviation was addressed to a Kohn anomaly [6] and a Peierl-like mechanism in metallic tubes, respectively. In addition Fig. 4 shows our results on the semiconducting (red x symbol) and metallic (blue plus symbol) nanotube. In case of the semiconducting nanotube we introduced an additional peak which is most obvious as a shoulder of the  $1590 \text{ cm}^{-1}$  peak when the nanotube is excited at  $2.039 \text{ eV}$  (bottom left of Fig. 2). Comparing the results presented in Ref. [7] to the experimental results in Ref. [8,21] shows that the theoretical values of the LO-phonons in semiconducting tubes underestimate the experimental values by  $\approx 10 \text{ cm}^{-1}$ . Therefore we can assign the peaks at  $1590 \text{ cm}^{-1}$  and  $1581 \text{ cm}^{-1}$  of to the LO and the TO phonon of the semiconducting nanotube. In case of the metallic nanotube (blue plus-symbol in Fig. 4) the theoretical values for the LO phonons (solid blue line) match our experimental finding of a broad peak at  $1540 \text{ cm}^{-1}$ . Our result supports the theory of a Kohn anomaly in metallic nanotubes.

In conclusion, we performed resonant Raman spectroscopy on a bundle of two nanotubes suspended in air. We showed that the lineshape of the high-energy modes, a sharp  $G^+$  peak at  $1590 \text{ cm}^{-1}$  and a broad asymmetric  $G^-$  peak at smaller wavenumbers, originate from different nanotubes. Including results from the radial breathing modes we assigned the sharp peak at  $1590 \text{ cm}^{-1}$  to a semiconducting and the broad peak at  $1540 \text{ cm}^{-1}$  to a metallic nanotube. Observing an asymmetric lineshape of the latter peak our results confirm the theory of a coupling of the phonons to a continuum of electronic states close to the Fermi-level. By comparison of the observed phonon frequencies to theoretical ones we assign both high-energy modes to LO phonons,  $G^+$  of the semiconducting tube and  $G^-$  of the metallic tube.

## References

- [1] R. Krupke et al., *Science* **301**, 344 (2003).
- [2] M. S. Strano et al., *Science* **301**, 1519 (2003).
- [3] M. Zheng et al., *Science* **302**, 1545 (2003).
- [4] A. Jorio et al., *Phys. Rev. B* **66**(11), 115411 (2002).
- [5] O. Dubay *et al.*, *Phys. Rev. Lett.* **88**, 235506 (2002).
- [6] M. Lazzeri et al., *Phys. Rev. B* **73**, 155426 (2006).
- [7] S. Piscanec et al., *Phys. Rev. B* **75**, 035427 (2007).
- [8] H. Telg et al., in: *Electronic Properties of Novel Nanostructures*, edited by H. Kuzmany, J. Fink, M. Mehring, and S. Roth, AIP Vol. 786 (American Institute of Physics, 2005), p. 162.
- [9] Y. Wu et al., *Phys. Rev. Lett.* **99**, 027402 (2007).
- [10] M. Oron-Carl et al., *Nano Lett.* **5**(9), 1761 (2005).
- [11] S. D. M. Brown et al., *Phys. Rev. B* **63**, 155414 (2001).
- [12] K. Kempa, *Phys. Rev. B* **66**, 195406 (2002).
- [13] M. Y. Sfeir et al., *Science* **306**, 1540 (2004).
- [14] H. Telg et al., *Phys. Rev. Lett.* **93**, 177401 (2004).
- [15] J. Maultzsch et al., *Phys. Rev. B* **72**, 205438 (2005).
- [16] V. N. Popov et al., *Phys. Rev. B* **72**, 035436 (2005).
- [17] C. Fantini et al., *Phys. Rev. Lett.* **93**, 147406 (2004).
- [18] M. O'Connell et al., *Phys. Rev. B* **69**, 235415 (2004).
- [19] C. Thomsen, *Light scattering in high- $T_c$  superconductors*, in: *Light Scattering in Solids VI*, Topics in Applied Physics, Vol. 68 (Springer-Verlag, Heidelberg, 1991), p. 285.
- [20] F. Cerdeira et al., *Phys. Rev. B* **8**(10), 4734 (1973).
- [21] M. Paillet et al., *Phys. Rev. Lett.* **96**, 257401 (2006).